



TITLE:

# Spontaneous formation of closed-field torus equilibrium via current jump observed in an electron-cyclotron-heated plasma

AUTHOR(S):

Yoshinaga, T; Uchida, M; Tanaka, H; Maekawa, T

---

CITATION:

Yoshinaga, T ...[et al]. Spontaneous formation of closed-field torus equilibrium via current jump observed in an electron-cyclotron-heated plasma. Physical Review Letters 2006, 96(12): 125005.

ISSUE DATE:

2006-03-31

URL:

<http://hdl.handle.net/2433/50248>

RIGHT:

Copyright 2006 American Physical Society

# Spontaneous Formation of Closed-Field Torus Equilibrium via Current Jump Observed in an Electron-Cyclotron-Heated Plasma

T. Yoshinaga, M. Uchida, H. Tanaka, and T. Maekawa

*Graduate School of Energy Science, Kyoto University, Kyoto 606-8502, Japan*

(Received 7 September 2005; published 31 March 2006)

Spontaneous current jump resulting in the formation of closed field equilibrium has been observed in electron-cyclotron-heated toroidal plasmas under steady external fields composed of a toroidal field and a relatively weak vertical field in the low aspect ratio torus experiment device. This bridges the gap between the open field equilibrium maintained by a pressure-driven current in the external field and the closed field equilibrium at a larger current. Experimental results and theoretical analyses suggest a current jump model that is based on the asymmetric electron confinement along the field line appearing upon simultaneous transitions of field topology and equilibrium.

DOI: 10.1103/PhysRevLett.96.125005

PACS numbers: 52.55.Fa, 52.35.Vd, 52.50.Sw

Toroidal plasma current is needed in tokamaks to keep the plasma loop in equilibrium and to form nested magnetic surfaces for confinement. Usually, it is initiated, ramped-up, and maintained by induction from a central solenoid. For the last several decades, intensive investigations have been conducted to start-up and maintain the plasma current by using various noninductive methods including radio frequency wave injections, beam injections, and helicity injections [1,2], aiming to remove the central solenoid from future tokamak reactors. Without the central solenoid, the structure of reactors can be greatly simplified. This is highly desirable in spherical tokamaks because of its limited central space [2,3].

Among the various phases of noninductive current drive, the start-up phase is the most dynamic since it involves changes of field topology, which would drastically affect the plasma equilibrium and confinement. When the equilibrium and confinement change, characteristics of current generation would also change. This would in turn affect the temporal evolution of field topology. Such dynamic processes accompanying changes of field topology are universal in both laboratory and space plasmas [4]. Therefore, investigation of the start-up process is not only important for successful start-up in tokamaks but is also of general interest.

Electron cyclotron (EC) heating has been effective for noninductive start-up, and in a number of experiments some plasma currents were observed in EC heated plasmas with external vertical field  $B_v$  [5–8]. Especially, those with steady  $B_v$  provide a simple situation and are suitable to investigate the start-up process, and it is remarkable that closed field equilibria can be obtained by EC heating under steady  $B_v$  as shown in CDX-U and DIII-D [7,8]. In these experiments the generated plasma current  $I_p$  changed with  $B_v$ . It attained a maximal value at a weak  $B_v$  level. At stronger  $B_v$  levels, it decreased inversely proportional to  $B_v$  consistent with the formula

$$I_p = 2\langle p \rangle S / R B_v, \quad (1)$$

which was predicted for the regime of open field equilibrium where the self-poloidal field produced by the plasma current was small compared with  $B_v$  [9]. Here,  $\langle p \rangle$  is the spatially averaged plasma pressure,  $S (= \pi a^2)$  the plasma cross section, and  $R$  the plasma major radius. Meanwhile, the  $B_v$  necessary to maintain the plasma loop in equilibrium is given by the Shafranov formula [10],

$$B_v = \frac{\mu_0 I_p}{4\pi R} \left( \ln \frac{8R}{a} + \frac{l_i}{2} - \frac{3}{2} + \beta_p \right), \quad (2)$$

where  $\beta_p = 2\mu_0 \langle p \rangle / B_a^2 = 8\pi^2 a^2 \langle p \rangle / \mu_0 I_p^2$  and  $B_a = \mu_0 I_p / 2\pi a$  is the self-poloidal field. Equation (1) is an approximation of Eq. (2) at smaller  $I_p$ , where the term with  $\beta_p$  is dominant, while equilibria at larger  $I_p$  shall obey Eq. (2). Although closed field equilibria have been obtained in previous experiments [7,8], this change of equilibrium characteristics has not been well understood. Here we report the experimental results showing that a spontaneous current jump bridges the open field equilibrium at smaller  $I_p$  and the closed field one at larger  $I_p$ . We also propose a current generation model for the current jump.

The experiments were carried out in the low aspect ratio torus experiment (LATE) device [11]. The vacuum chamber is a cylinder with a diameter of 1.0 m and a height of 1.0 m [see Fig. 1(s)]. The center post with an outer diameter of 11.4 cm encloses 60 turns of conductors for the toroidal field. Four sets of poloidal field coils produce the external vertical field. There is no central solenoid for inductive current drive. Three 2.45 GHz magnetrons and a 5 GHz klystron were used for EC heating. In all cases, microwaves were injected from radial ports with injection angles slightly deviated (about 15°) from normal to the toroidal field.

Figure 1 shows a discharge by a 5 GHz microwave pulse under an external vertical field of  $B_v = 85$  G with a decay index of  $n = 0.1$  and a toroidal field of  $B_t = 720$  G (all at  $R = 25$  cm). The evolution of the plasma image on the video camera shows that breakdown takes place near the fundamental EC resonance layer at  $R = 10$  cm and the

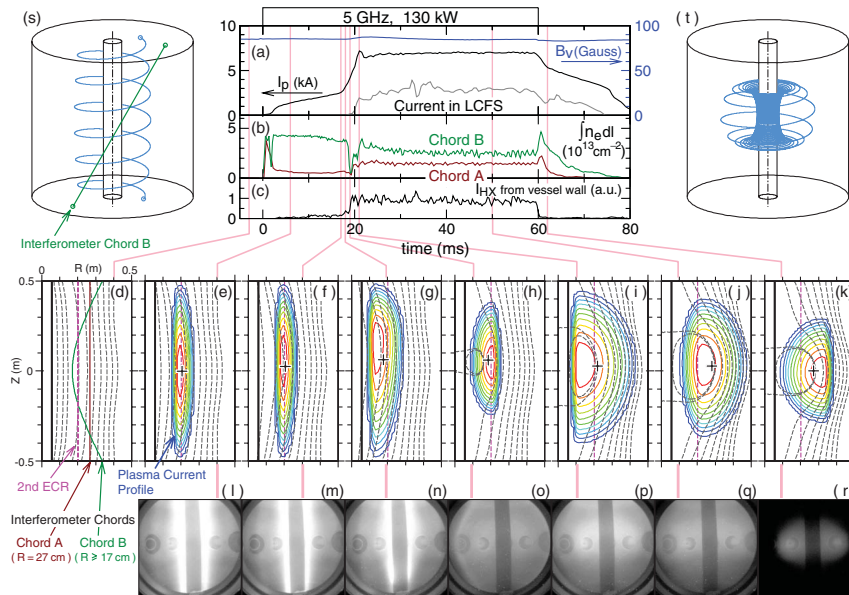


FIG. 1 (color). Time evolution of typical discharge. (a) Plasma current, (b) line densities, (c) hard x-ray intensity, (d)–(k) contour plots of current distribution and poloidal flux (the center of the plasma current is denoted by +), (l)–(r) visible light plasma images. Three-dimensional field lines for the cases of (d) and (j) are shown in (s) and (t), respectively.

plasma expands to the lower field side in a few milliseconds. In accordance with the plasma expansion, a plasma current is initiated and grows slowly up to 2.3 kA as shown in Fig. 1(a). Then the current suddenly increases (current jump) and reaches 7.0 kA, after which it is steady to the end of the microwave pulse.

Evolutions of the plasma current profile and the poloidal flux surface were analyzed by using the magnetic data from 13 flux loops with taking into account the eddy currents induced in the vessel walls [12] and displayed in Figs. 1(d)–1(k). Here, we employed a model current profile similar to that used in [11]. The profiles before the current jump are stretched vertically near the second harmonic resonance layer at  $R = 20$  cm [Figs. 1(e) and 1(f)]. When the current jump starts, it shifts to the higher field side [Fig. 1(g)] and a small closed flux surface touching the center post appears [Fig. 1(h)]. Then the current profile as well as the closed flux surface expands toward the vessel wall [Fig. 1(i)]. At the final steady stage, the current profile is detached from the center post and a large closed flux surface in the shape of low aspect ratio is formed [Fig. 1(j)]. It is remarkable that the open field configuration changes spontaneously into a closed field one by EC heating alone as shown in Figs. 1(s) and 1(t). The hard x-ray signal from the vessel wall [Fig. 1(c)], indicating the presence of an energetic electron tail beyond 100 keV, is strongly enhanced when the current profile expands near to the vessel wall. After the microwave is turned off the current decays and closed flux surface shrinks toward the center post under the steady  $B_v$  field [Fig. 1(k)]. The plasma images shown in Figs. 1(l)–1(r) correspond to Figs. 1(e)–1(k), respectively, and reflect the changes of field topology.

The current profile in the final stage [Fig. 1(j)] encompasses the second to fourth harmonic EC resonance layers. The line averaged electron density estimated from two chord signals at  $R \geq 17$  cm and  $R = 27$  cm [Fig. 1(b)]

are about  $6 \times 10^{11} \text{ cm}^{-3}$  and  $4 \times 10^{11} \text{ cm}^{-3}$ , respectively, exceeding the plasma cutoff density of  $3.1 \times 10^{11} \text{ cm}^{-3}$ . These results suggest that electron Bernstein waves (EBW) mode-converted from electromagnetic waves maintain the plasma. EBW is an electrostatic mode and its absorption is significant even at harmonic resonances, while the absorption of the electromagnetic modes is quite weak in the present low temperature plasma.

Formation of closed field equilibrium via current jump has been observed for a wide range of  $B_v$  in both 2.45 and 5 GHz experiments as shown in Fig. 2. All the characteristic currents including the current just before current jump  $I_{jbf}$ , the current at which initial closed surface appears  $I_{ics}$ , and the final current after current jump  $I_{finl}$  are roughly proportional to  $B_v$ . For each  $B_v$ , there is a threshold microwave power  $P_{rth}$ , over which the plasma current can reach  $I_{jbf}$  and current jump takes place. Even when microwave power  $P_{rf}$  is larger than  $P_{rth}$ , none of these characteristic currents change. In this case, only the time needed for  $I_p$  to reach  $I_{jbf}$  decreases. These results suggest that current jump takes place when the deformation of the field structure due to the self field from the plasma current reaches a certain level.

The plasma loop may be at equilibrium for radial force balance even during the current jump since its characteristic time is much longer than the Alfvén and ion sound transit times (several microseconds). For the sake of simplicity, we consider equilibrium by using Eq. (2). The formula can be cast into the dimensionless form

$$\bar{B}_v = \left( \ln \frac{8R}{a} + \frac{l_i}{2} - \frac{3}{2} \right) \bar{I}_p + \frac{1}{\bar{I}_p}, \quad (3)$$

where  $\bar{B}_v = \sqrt{\frac{2}{\mu_0}} \frac{(R/a)B_v}{\sqrt{\langle p \rangle}}$ , and  $\bar{I}_p = \sqrt{\frac{\mu_0}{8}} \frac{I_p}{\pi a \sqrt{\langle p \rangle}}$ . Here, the first term is proportional to  $I_p$  and is responsible for the current-hoop force and the second term is inversely pro-

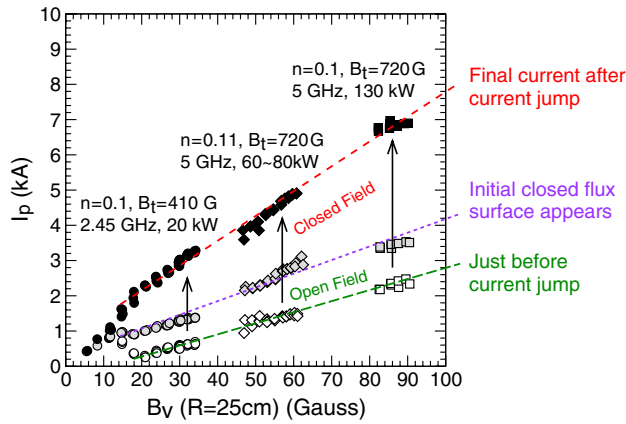


FIG. 2 (color online). Various characteristic currents for current jump versus  $B_v$ .

portional to  $I_p$  and responsible for the pressure-ballooning force. The equilibrium characteristics for various aspect ratios  $R/a$  are plotted in Fig. 3. Two terms in Eq. (3) balance at the pressure-current (PC) turning point in this figure and the lower part from this point is the pressure-ballooning-force dominating regime and the upper part is the current-hoop-force dominating regime.

The ratio of the self-poloidal field to the external vertical field,  $B_a/B_v$ , is a measure of the deformation of the poloidal field from the external field. When  $I_p$  increases and  $B_a$  becomes comparable to  $B_v$ , closed flux surfaces appear. The point where  $B_a = B_v$  is near the PC turning point when the aspect ratio is low as shown in Fig. 3. This result and the results shown in Fig. 2 suggest that the plasmas before current jump are in the pressure-ballooning-force dominating regime and the plasmas after current jump are in the current-hoop-force dominating regime. The current jump bridges both regimes. Furthermore, it has been confirmed in both 2.45 and 5 GHz experiments that once a large closed flux surface is formed via current jump,  $I_p$  can be further ramped-up by increasing  $P_{rf}$  with a  $B_v$  ramp for

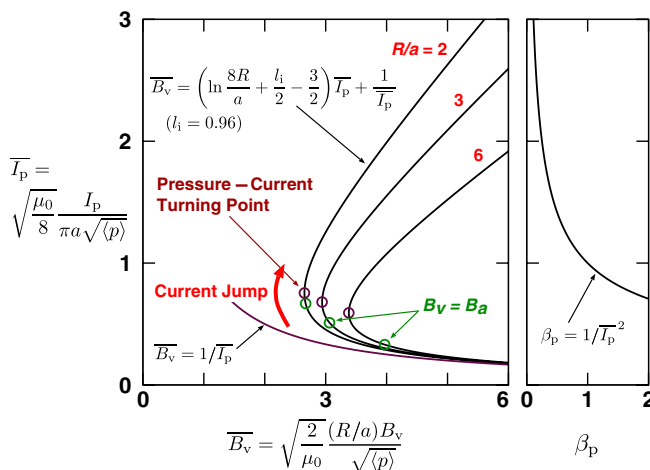


FIG. 3 (color online). Equilibrium characteristics for various aspect ratios.

equilibrium of the plasma loop at larger currents [11], being consistent with the above picture.

The equilibrium characteristics predict that  $I_p$  at the initial discharge stage where  $I_p$  is very small is given by  $\bar{I}_p = 1/\bar{B}_p$ , or  $I_p = 2\pi a^2 \langle p \rangle / RB_v$ , as mentioned in the introduction. This has been confirmed in a 2.45 GHz experiment at a low microwave power of  $P_{rf} = 5$  kW, where Langmuir probe measurement was possible.  $I_p$  at the initial discharge stage much before the current jump is proportional to electron pressure and inversely proportional to  $B_v$ , as shown in Figs. 4(a) and 4(d), respectively. This is the return current along the helical field line [see Fig. 1(s)] that cancels the charge separation due to the  $\nabla B$  and curvature drifts [9]. It is noted that  $I_p$  in Fig. 4(a) deviates from the relationship of  $\bar{I}_p = 1/\bar{B}_v$  near the current jump, being consistent with the characteristics shown in Fig. 3.

The equilibrium characteristics indicate that  $\bar{B}_v$  is constant when  $\bar{I}_p$  increases through the PC turning point. This implies that an efficient current generation in the sense of current increment with very small increments of plasma pressure is required for the transition through the PC turning point (Note that  $B_v$  is steady in the experiments). This current generation may be related to the change of field structure from an open to a closed one [5].

We consider the single particle orbit of electrons. The vertical drift velocity of electrons in the external fields of  $B_v$  and  $B_t$  is given by  $v_z = v_{||}(B_v/B_t) - m(v_{||}^2 + v_{\perp}^2/2)/eRB_t$ . When  $v_z = 0$ , the electrons make a circular orbit along the toroidal field on the equatorial plane. This condition makes an ellipse in the velocity space;  $(v_{||} - g/2)^2 + v_{\perp}^2 = (g/2)^2$ , where  $g = eRB_v/m$ . This  $v_z = 0$  ellipse is located on the side of the current carrying electrons in the velocity space, manifesting current generation by means of the asymmetric confinement [13].

In order to investigate the electron confinement in the presence of the self field, the electron orbits, which start at the vessel center at various velocities and pitch angles, are

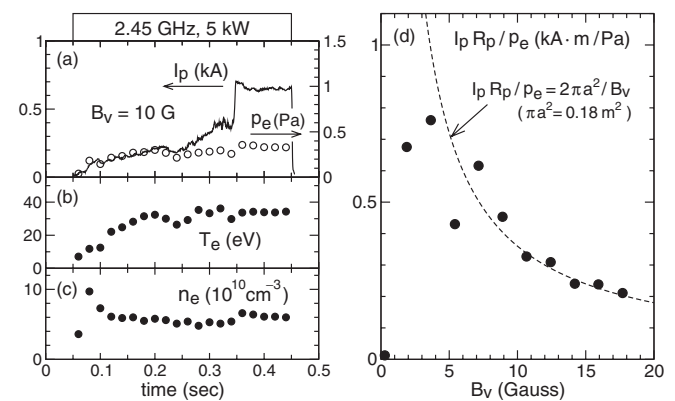


FIG. 4. (a) Temporal evolutions of plasma current ( $I_p$ ), electron pressure ( $p_e$ ), (b) electron temperature ( $T_e$ ), and (c) density ( $n_e$ ). (d) Relationship of  $I_p R_p / p_e$  versus  $B_v$  at the initial discharge stage.  $R_p$  is the plasma major radius.



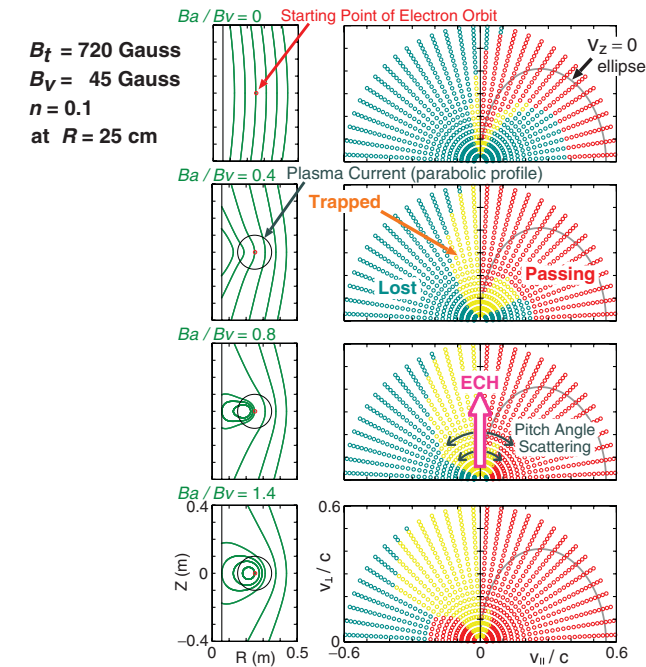


FIG. 5 (color). Poloidal flux surfaces and confined areas in the velocity space for various levels of the self field.

numerically investigated as shown in Fig. 5. Because of the mirror shaped  $B_v$  field, some electrons around the  $v_z = 0$  ellipse are also confined (trapped and passing) in the external field in the sense that their orbits do not cross the vessel wall. These selectively confined passing electrons are provided from the thermal bulk by the perpendicular EC heating (ECH) and subsequent pitch angle diffusion. Their population may be, however, quite few in this stage. The asymmetric passing area expands towards the lower energy range as the self field  $B_a$  from the pressure-driven current increases. When  $B_a$  increases to a certain level, the passing area front reaches the peripheral region around the thermal bulk (say, keV range). Here, the current generation due to the asymmetric confinement would begin in full scale since the electron population becomes significant and the pitch angle scattering becomes frequent near the thermal bulk. The resultant current increase enlarges the passing area further and current increase would be quickly accelerated since both the electron population and pitch angle diffusion rate increase drastically towards the thermal bulk, resulting in the current jump. The pressure increment is most small when currents are carried by these unidirectional lower energy electrons, meeting the equilibrium requirement for the PC transition. Furthermore, the  $90^\circ$  scattering time for 1 keV electrons estimated for the present density ( $5 \times 10^{11} \text{ cm}^{-3}$ ) is 1.3 ms, being consistent with the experimental current jump time. Such a filling of passing area toward the lower energy range takes place first at the inboard side of the current loop, where deformation of

the field is stronger compared with the outboard side as shown in Fig. 5, being consistent with the experimental results shown in Figs. 1(f)–1(j). After  $B_a \sim B_v$ , the EC current drive can become effective since forward electrons are all confined.

As shown in Figs. 1(a) and 1(j) a large fraction of the current (60%) still flows in the open field area outside the last closed flux surface (LCFS) even after the current jump. This current may be generated by the toroidal precession of trapped electrons enhanced by EC heating under large mirror ratios of this area in the low aspect ratio configuration [8]. The outward shift of energetic passing electron orbits from LCFS can also contribute to the current since the poloidal Larmor radius is still large ( $\sim 5 \text{ cm}$  for 10 keV electron) at  $I_p = 7 \text{ kA}$ . On closed flux surfaces there may also be a significant trapped-electron driven current in addition to the EC-driven current since  $\beta_p \sim 1$  as inferred from Fig. 3. In a discharge, where  $B_v$  was ramped-up for equilibrium at larger currents, the current fraction inside LCFS was observed to increase to 66% in accordance with the expansion of LCFS as the current increased to  $I_p = 12 \text{ kA}$ .

Interestingly, as the aspect ratio becomes low, the point where  $B_a = B_v$  approaches the PC turning point on the equilibrium characteristic curves as shown in Fig. 3, that is, both transitions in field topology (from open to closed fields) and equilibrium (from pressure ballooning to current hoop) coincide. The equilibrium characteristics predict that when  $R/a$  is strictly fixed, a current increment with no pressure increment is required for the transition through the PC turning point. This seems to be impossible. Some changes of  $R/a$ , that is, a decrease of  $R/a$  just before the PC turning point and an increase of  $R/a$  at and after the PC point, may assist the transition as inferred from Fig. 3 and seen in Figs. 1(f)–1(j).

- [1] N. J. Fisch, Rev. Mod. Phys. **59**, 175 (1987).
- [2] Y.-K. M. Peng, in *Proceedings of the 20th International Conference on Fusion Energy, Vilamoura, 2004* (IAEA, Vienna, 2004), FT/3-1Rb.
- [3] R. Raman *et al.*, Phys. Rev. Lett. **90**, 075005 (2003).
- [4] E. Priest and T. Forbes, in *Magnetic Reconnection* (Cambridge University Press, Cambridge, England, 2000).
- [5] T. Shimozuma *et al.*, J. Phys. Soc. Jpn. **54**, 1360 (1985).
- [6] S. Tanaka *et al.*, Nucl. Fusion **33**, 505 (1993).
- [7] C. B. Forest *et al.*, Phys. Rev. Lett. **68**, 3559 (1992).
- [8] C. B. Forest *et al.*, Phys. Plasmas **1**, 1568 (1994).
- [9] L. E. Zakharov and G. V. Pereverzev, Sov. J. Plasma Phys. **14**, 75 (1988).
- [10] V. D. Shafranov, in *Review of Plasma Physics* (Consultants Bureau, New York, 1966), Vol. 2.
- [11] T. Maekawa *et al.*, Nucl. Fusion **45**, 1439 (2005).
- [12] Y. S. Hwang *et al.*, Rev. Sci. Instrum. **63**, 4747 (1992).
- [13] K.-L. Wong *et al.*, Phys. Rev. Lett. **45**, 117 (1980).